One-sided oxidation tests were conducted with as-fabricated and high-burnup 9×9 Zry-2 (see Tables 3 and 7 for material parameters) to determine the oxidation kinetics [15]. Tests were conducted at 1000ºC (1200-6000 s), 1100ºC (600-3000 s), and 1204ºC (300-1200 s). Measured weight gain based on the increase in sample weight tended to be higher than CP-predictions due to some steam leakage causing inner-surface oxidation near the sample ends for all three oxidation temperatures. The weight-gain results based on metallographic images and analysis were in excellent agreement with the CP-predicted weight gains for the 1204ºC-oxidized samples. The measured oxide layer thicknesses were also in excellent agreement with the CP-predicted oxide layer thicknesses (see page 74 of Ref. 13). However, the measured oxygen-stabilized-alpha layer thicknesses were as much as 40% higher than the CP-predicted values. This is important in evaluating the use of the CP-correlations in deducing beta-layer thickness vs. time at temperature. In the ANL tests, the argon purge flowing through the inside of the samples minimized hydrogen pickup (<50 wppm) from inner-surface oxidation and allowed desorption of hydrogen from the beta layer to the purge. According to Cathcart et al. (Ref. 3, Appendix B, Table B1, page 166), samples oxidized (one-sided) at 1203ºC for only 236 s picked up 250-450 wppm hydrogen. Samples oxidized at lower temperatures for longer times picked up as much as 750-wppm hydrogen. Hydrogen is a beta-stabilizer, which results in a decrease in alpha layer thickness and an increase in beta-layer thickness. Figure 40 [22] shows the comparison of the ANL measured (alpha + oxide)-layer thickness and the CP-predicted (alpha + oxide)-layer thickness. The higher measured values are due to the higher measured values for the alpha-layer thickness.

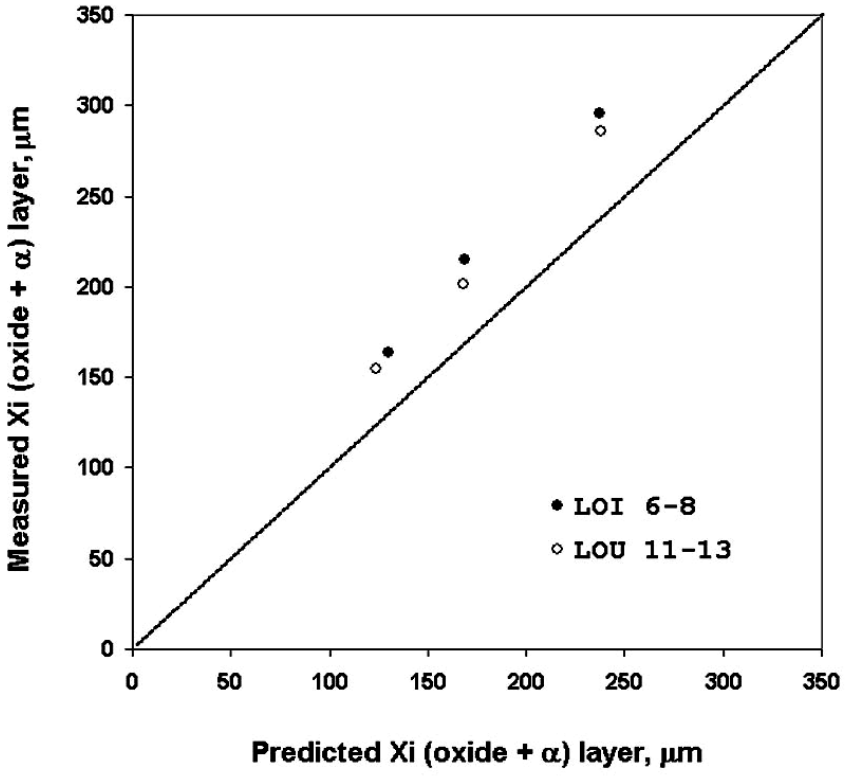

Figure 40. Measured vs. CP-model-predicted Xi (oxide + alpha) layers after steam-oxidation tests (300, 600 and 1200 s at ≈1204°C) with irradiated (LOI 6-8) and unirradiated (LOU 11-13) Zry-2.

3.2.1 Post-quench ductility of 10×10 Zry-2 oxidized at 1000ºC and 1200ºC

10×10 Zry-2 Oxidized at 1000ºC

10×10 Zry-2 cladding samples were oxidized (two-sided) at 1000˚C to 10%, 13% and 17% CP-ECR. Thermal benchmark results are shown in Figure 41. For the oxidation tests, the control thermal couple was lowered by 5ºC to give an average hold temperature of 1004±7ºC up to 2000 s and a long-time (≥2000 s) hold temperature of 1000±8ºC. Following the heating phase, samples were cooled from 1000˚C to 800˚C at ≈10˚C/s, quenched and ring-compressed at RT. An additional test at 20.7% CP-ECR was performed without quench for the breakaway oxidation studies (see 3.2.2). The weight gain and post-test ductility for this sample are included in this section.

As-fabricated Zry-2 rings were compressed to 2-mm displacement and to maximum displacement. The thin-ring analytical solution for loading stiffness of a homogeneous Zry-2 wall is 1.06 kN/mm. The stiffness determined from the load-displacement curve was 0.95 kN/mm. The measured value is ≈10% lower than the predicted value, which is reasonable because: the Zr-liner may have a lower elastic modulus than Zry-2; an isotropic approximation for the elastic modulus of Zry-4 was used; and machine compliance may cause a reduction in stiffness. The difference between offset (1.54 mm) and permanent (1.39 mm) displacements was 0.15 mm, which is consistent with other cladding alloys tested. The maximum offset strain that can be achieved with this cladding geometry is 60%.

The weight gains listed in Table 21 for the 1000ºC-oxidized Zry-2 cladding are significantly lower than the CP-predicted weight gains and the measured weight gains for 17×17 Zry-4 (see Table 9 for Zry-4 results). Figure 42 shows the comparison. As indicated in Table 9, Zry-2 cladding has a Zr liner on the inner surface, which is about 10% of the wall thickness. Previous outer-surface oxidation tests conducted with 9×9 Zry-2 indicated excellent agreement between Zry-2 measured and predicted weight gains and oxide layer thicknesses. Quantitative metallography was performed for the Zry-2 sample used to generate the temperature history shown in Figure 41 (2000 s from ramp initiation to end of heating phase at 1000ºC; ≈13% CP-ECR). The outer- and inner-surface oxide layers were 52±2 μm and 31±2 μm, respectively. The circumferential uniformity of oxide layer thickness indicates very little temperature variation. More significantly, the decrease of ≈40% in inner-surface oxide layer relative to outer-surface oxide layer and CP-predicted oxide layer thickness explains the lower-than-predicted weight gain. Figure 43 shows metallographic images of the sample oxidized to 10% CP-ECR: (a) one of eight cross-sectional arc lengths; (b) Zry-2 outer surface; and (c) the Zr-lined inner surface. The interface between the prior-beta-phase Zr-liner and Zry-2 is apparent in Figure 44c.

The ring-compression test results of the 1000ºC-oxided Zry-2 cladding are also summarized in Table 21. The post-quench ductility of 10×10 Zry-2 is higher than the ductility of 17×17 Zry-4 oxidized at 1000ºC to 17% CP-ECR: 12±2% vs. 5.1% offset strain, respectively. Based on the 20.7% CP-ECR sample that was not quenched, Zry-2 oxidized at 1000ºC retains RT post-quench ductility at >20% CP-ECR. It is interesting to note that through-wall failure for two-sided-oxidized Zry-2 cladding rings appears as likely to initiate at the outer Zry-2 surface at ±90º from the loading direction as at the inner Zr surface along the loading direction. The 20.7% CP-ECR sample developed one through-wall crack at 90º from the loading direction (side wall) and a second nearly-through-wall crack along the loading direction at the bottom surface. The results suggest that the oxygen-stabilized alpha layer formed within the Zr-liner may not be as brittle as the oxygen-stabilized alpha layer formed within the Zry-2 cladding.

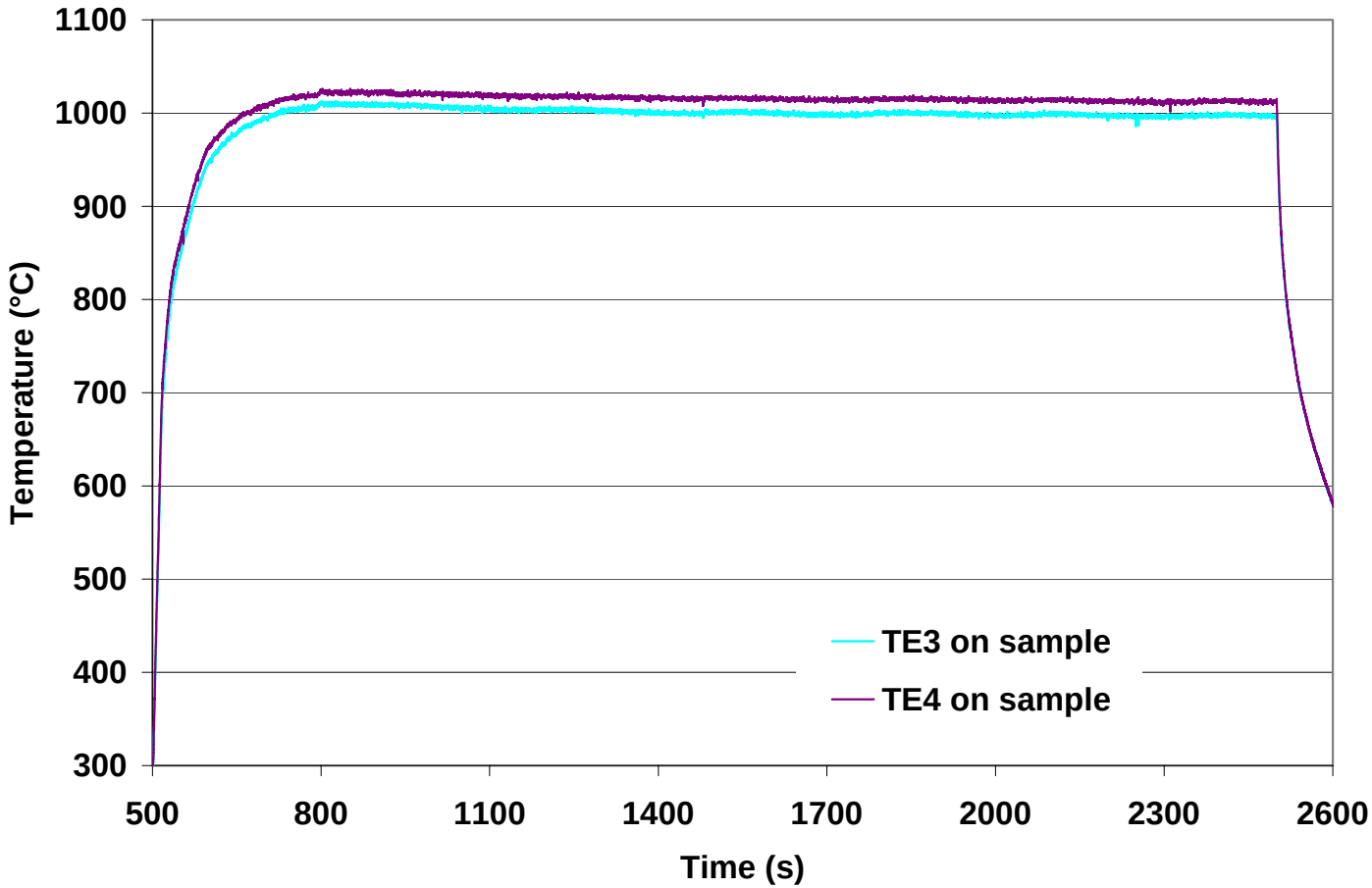

Figure 41. Thermal benchmark results for 10×10 Zry-2 at 1000ºC target temperature. Average hold temperature is 1009±7ºC. Hold temperature after 2000 s from ramp initiation is 1005±8ºC. For oxidation tests, the control TC was lowered by ≈5ºC to give a long-time hold temperature of 1000±8ºC.

Table 21 Ring Compression Test (RCT) Results for 10×10 Zry-2 Cladding Oxidized at 1000˚C, Cooled at ≈10˚C/s to 800˚C and Quenched. ECR = 1.328 Wg for 0.66-mm-wall cladding. Tests were performed on ≈8-mm-long samples at RT and 0.0333 mm/s displacement rate. Displacements in the loading direction were normalized to the as-fabricated outer diameter (10.29 mm) to calculate strains.

Test Conditions			ECR %		Plastic Displacement mm		Plastic Strain %	
T, ˚C		Test Time[a] s	CP	Meas.	Offset	Permanent	Offset	Permanent
Ox.	RCT							
---	RT	--	0	0	6.0	---	60	---
1000	RT	1150	10.0	8.0	≥5.1 <6.6	≥5.1 ---	≥46 <64	≥40
1000	RT	1930	13.0	10.4	>1.16 4.81	>0.89 3.46	>11 47	>8.8 34
1000	RT	3420	17.0	13.6	1.48 0.95	1.28 0.55	14 9.2	12 5.3
1000[b]	RT	5000	20.7	15.6	0.65	<0.5	6.3	<5

[a]Includes time for ramp from 300ºC and hold time.
[b]Breakaway oxidation test conducted with cooling from 1000ºC to RT without quench.

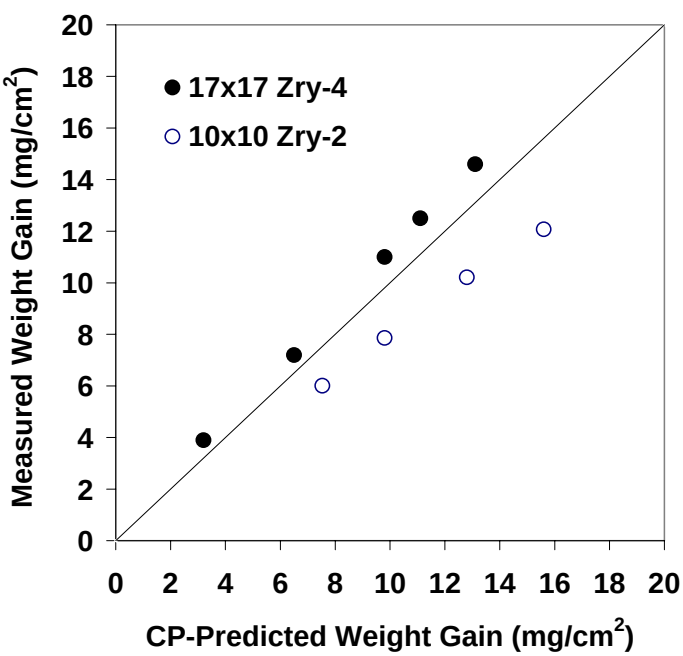

Figure 42. Comparison of measured and CP-predicted weight gains for Zr-lined 10x10 Zry-2 and 17x17 Zry-4 oxidized at 1000ºC.

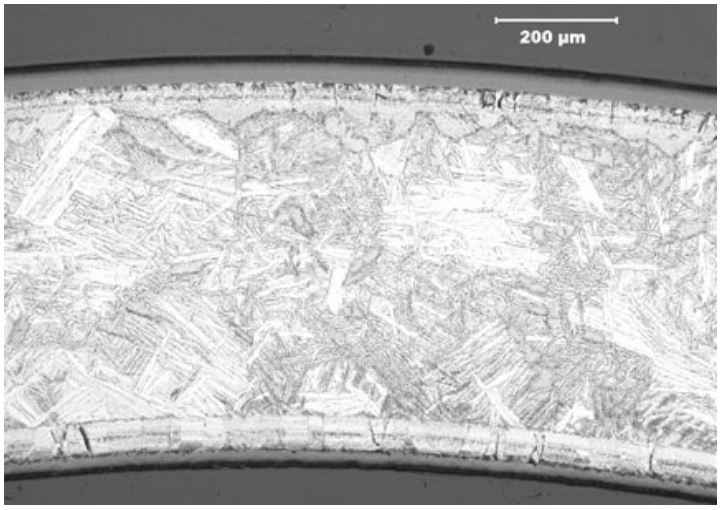

(a) Cross section

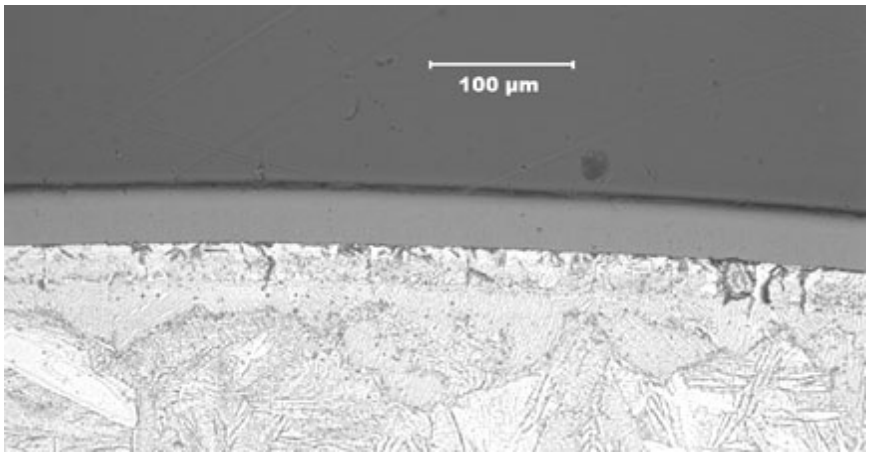

(b) Outer Zry-2 surface

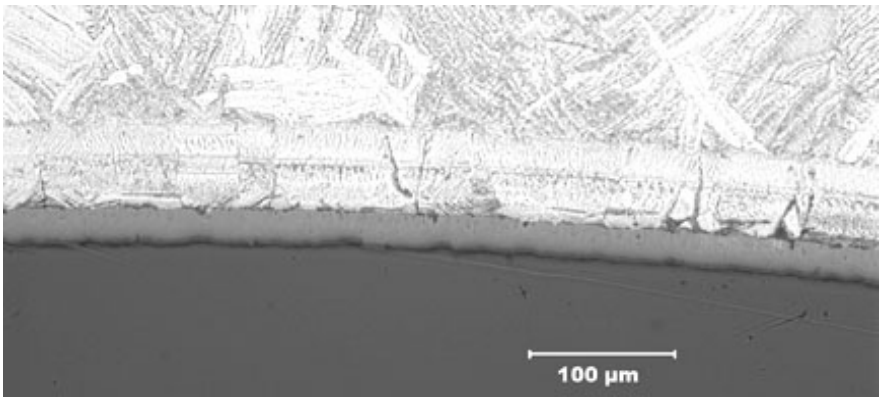

(b) Inner Zr-lined surface

Figure 43. 10×10 Zry-2 sample oxidized at 1000ºC to 10% CP-ECR: (a) one of eight cross-sectional arc lengths; (b) outer Zry-2 surface, and inner Zr-liner surface.

10×10 Zry-2 Oxidized at 1200ºC

10×10 Zry-2 cladding samples were oxidized (two-sided) at 1200˚C to 10%, 13%, 17% and 20% CP-ECR. Thermal benchmark results are shown in Figure 44. Following the heating phase, samples were cooled from 1200˚C to 800˚C at ≈13˚C/s, quenched and ring-compressed at 135˚C.

As-fabricated Zry-2 rings were compressed at 135˚C to 2-mm and to maximum displacement. The thin-ring analytical solution at 135˚C for loading stiffness of a homogeneous Zry-2 wall is 0.98 kN/mm. The stiffness determined from the load-displacement curve was 0.81 kN/mm. The results suggest that the elastic modulus of the Zry-2/Zr composite may decrease more than the predicted 7.5% fro Zry-4 from RT to 135˚C. The difference between offset (1.65 mm) and permanent (1.52 mm) displacements was 0.13 mm, which is consistent with the RT results. The maximum offset strain that can be achieved with this cladding geometry and the thermocouple on the inner-surface of the cladding is 50%.

The weight gains listed in Table 22 for the 1200ºC-oxidized Zry-2 cladding are in good agreement with the CP-predicted weight gains and the measured weight gains for 17×17 Zry-4 (see Table 9 for Zry-4 results). Figure 45 shows the comparison. Although the measured weight gains are in good agreement, the oxide layer on the Zr liner is ≈15% thinner than the oxide layer on the Zry-2 outer surface. Quantitative metallography was performed on the Zry-2 cladding sample exposed to the temperature history shown in Figure 44 (≈17% CP-ECR). The measured outer- and inner-surface oxide layers were 62±2 μm and 53±2 μm, respectively. As with the 1000ºC-oxidized sample, the small circumferential variation in oxide thicknesses indicates very good temperature uniformity. Micrographic images in Figures 46 (170-s and 10% CP-ECR) and 47 (423 s and 17% CP-ECR) show the differences in oxide layer thicknesses. Also, the oxygen-stabilized alpha layers, which are predicted to be about the same thickness as the oxide layers, are significantly thicker than predicted for both surfaces. Based on the results in Figure 46c and 47c, the Zr-liner (≈66-μm thick) has been consumed by oxidation and transformation to oxygen-stabilized alpha for ≥10% CP-ECR (≥170-s test time) at 1200ºC.

The ring-compression tests results for 1200ºC-oxided Zry-2 cladding rings are also summarized in Table 22. The transition CP-ECR is ≈19% based on interpolation. Although the transition value falls within the range measured for two types of Zry-4, the decrease in ductility with increasing CP-ECR for Zry-2 is clearly more gradual than the trend curves for Zry-4. Comparison of the Zry-2 and Zry-4 post-quench-ductility results is shown in Figure 48. This gradual decrease in ductility with CP-ECR may be due to the presence of the liner. For homogeneous Zry-4, the growth of the brittle oxide- and oxygen-stabilized-alpha layers is expected to be the same at the inner and outer surfaces. Also, the rate of oxygen diffusion into the beta layer is expected to be the same from the outer- and inner-surfaces of the beta layer. As such, through-wall failure of the compressed ring should initiate at the cladding inner surface under the loading plate or above the support plate. For 1200ºC-oxidized Zry-2 cladding at 10% and 13% CP-ECR, through-wall failure was observed at the side of the sample, 90º from the loading direction. At the side locations, the maximum tensile bending stress is located at the cladding outer surface. The 17% CP-ECR samples failed with multiple through-wall cracks: top, 45º, and side for one sample; and bottom and 45º for the second sample. The 20% CP-ECR samples failed in the traditional manner with a single through-wall crack at either the top or bottom of the ring.

Chung and Kassner [18] measured the oxygen content (2.5 wt.%) needed to stabilize alpha in Zry-4 at 1200ºC. They also reviewed previous studies with zirconium, for which 2.1-2.2 wt.% oxygen is sufficient to stabilize alpha in Zr at 1200ºC. Based on these studies and on the ring compression results, it appears that the Zry-2 oxygen-stabilized alpha layer is more brittle than the Zr-liner alpha layer although both layers would be classified as brittle.

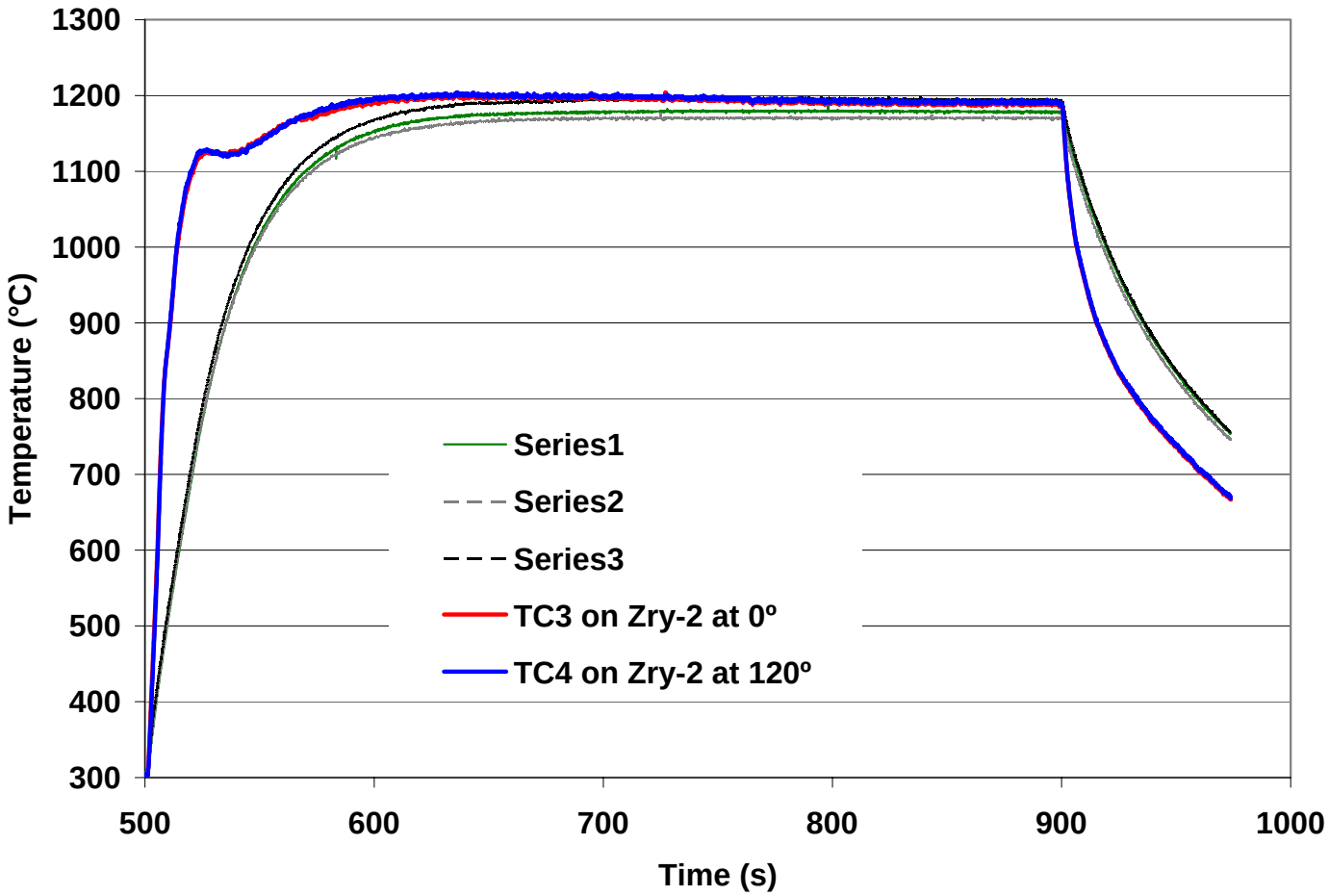

Figure 44. Thermal history for 10×10 Zry-2 oxidation tests at 1200±6ºC. The raw data for the sample TC readings were corrected based on calibrating these TCs to an ANL NIST-calibrated TC. Also shown are the three TC readings for the holder TCs (Series 1-3).

Table 22 Ring Compression Test (RCT) Results for 10×10 Zry-2 Cladding Oxidized at 1200˚C, Cooled at ≈13˚C/s to 800˚C and Quenched. ECR = 1.328 Wg for 0.66-mm-wall cladding. Tests were performed on ≈8-mm-long samples at 135˚C and 0.0333 mm/s displacement rate. Displacements in the loading direction were normalized to the as-fabricated outer diameter (10.29 mm) to calculate strains.

Test Conditions			ECR %		Plastic Displacement, mm		Plastic Strain, %	
T, ˚C		Test Time[a] s	CP	Meas.	Offset	Permanent	Offset	Permanent
Ox.	RCT							
---	135	---	0	0	5.11	5.18	50	50
1200	135	170	10.0	10.8	2.48 2.60	2.12 2.27	24 25	21 22
1200	135	260	13.0	13.7	1.12 1.44	--- 1.34	11 14	--- 13
1200	135	423	17.0	17.1	0.75 0.56	--- 0.29	7.3 5.4	--- 2.8
1200	135	575	20.0	19.9	0.19 0.15	0.09 0.10	1.9 1.5	0.9 1.0

[a]Includes time for ramp from 300ºC and hold time.

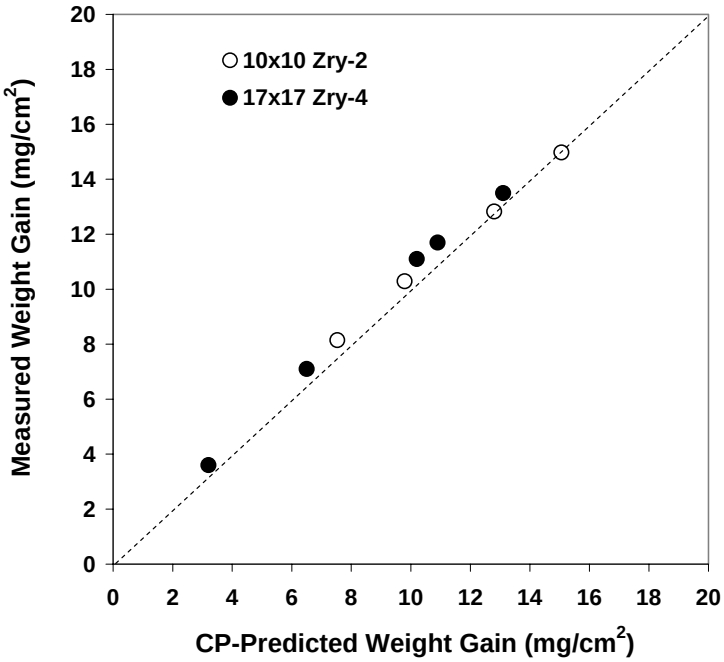

Figure 45. Comparison of measured and CP-predicted weight gains for 10x10 Zry-2 and 17x17 Zry-4 oxidized at 1200ºC, cooled at ≈13ºC/s to 800ºC, and quenched at 800ºC.

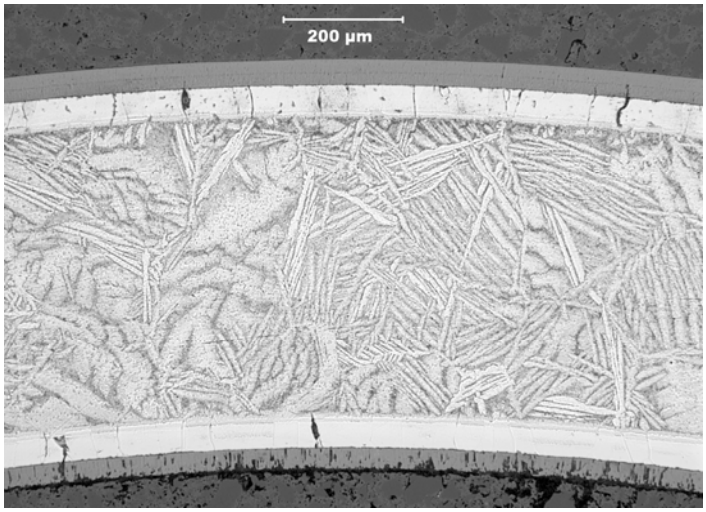

(a) Cross section

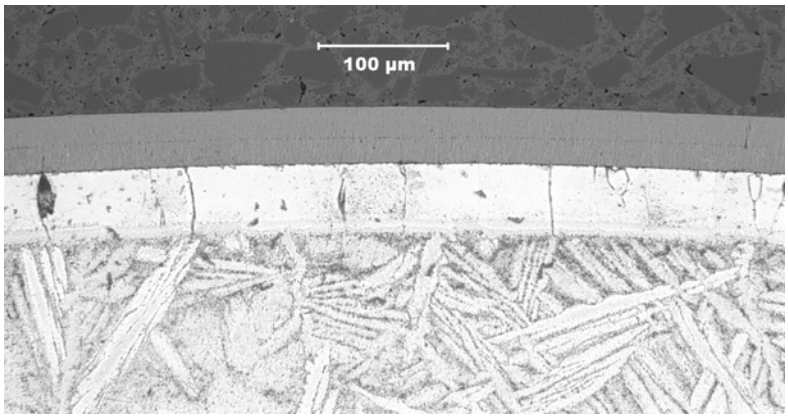

(b) Outer Zry-2 surface

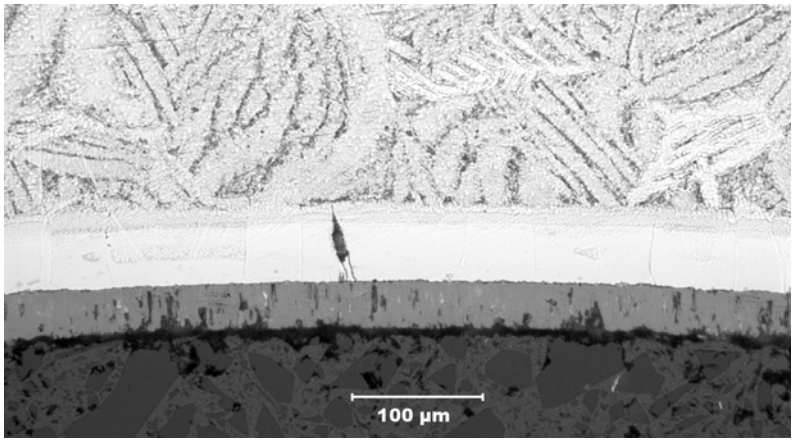

(c) Inner Zr-lined surface

Figure 46. Metallographic images of 10×10 Zry-2 sample oxidized at 1200ºC to 10% CP-ECR: (a) cross section (one of 8 orientations); (b) outer Zry-2 surface; and (c) inner Zr-lined surface.

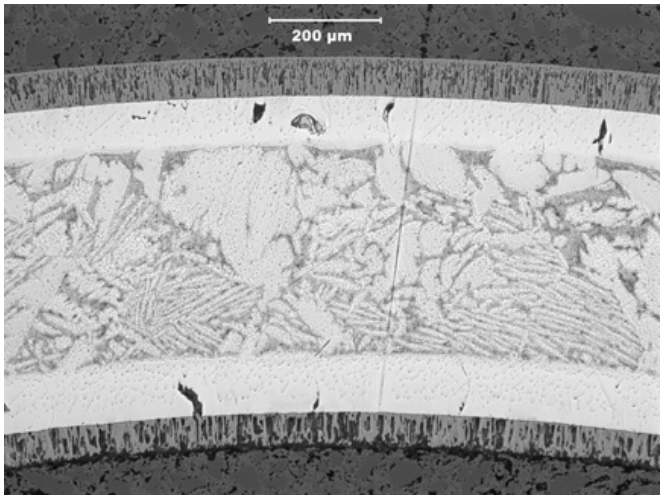

(a) Cross section

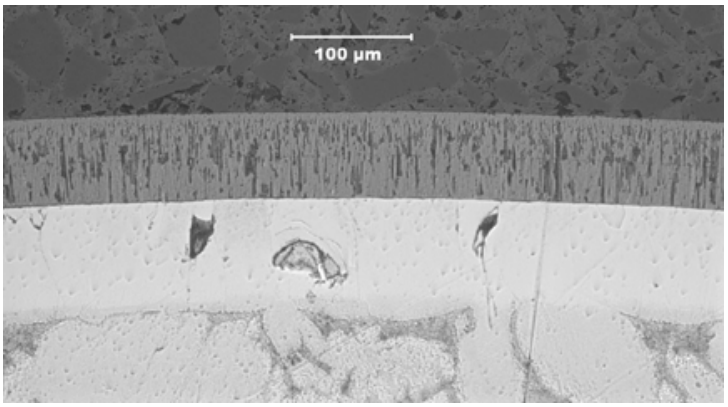

(b) Outer Zry-2 surface

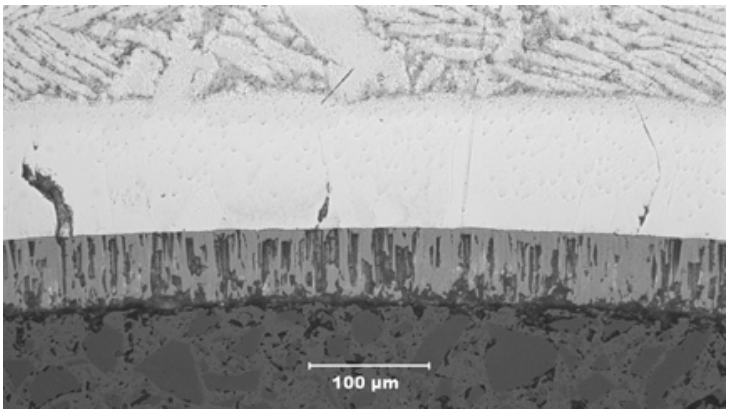

(c) Inner Zr-lined surface

Figure 47. Metallographic images of 10×10 Zry-2 sample oxidized at 1200ºC to 17% CP-ECR: (a) cross section (one of 8 orientations); (b) outer Zry-2 surface; and (c) inner Zr-lined surface

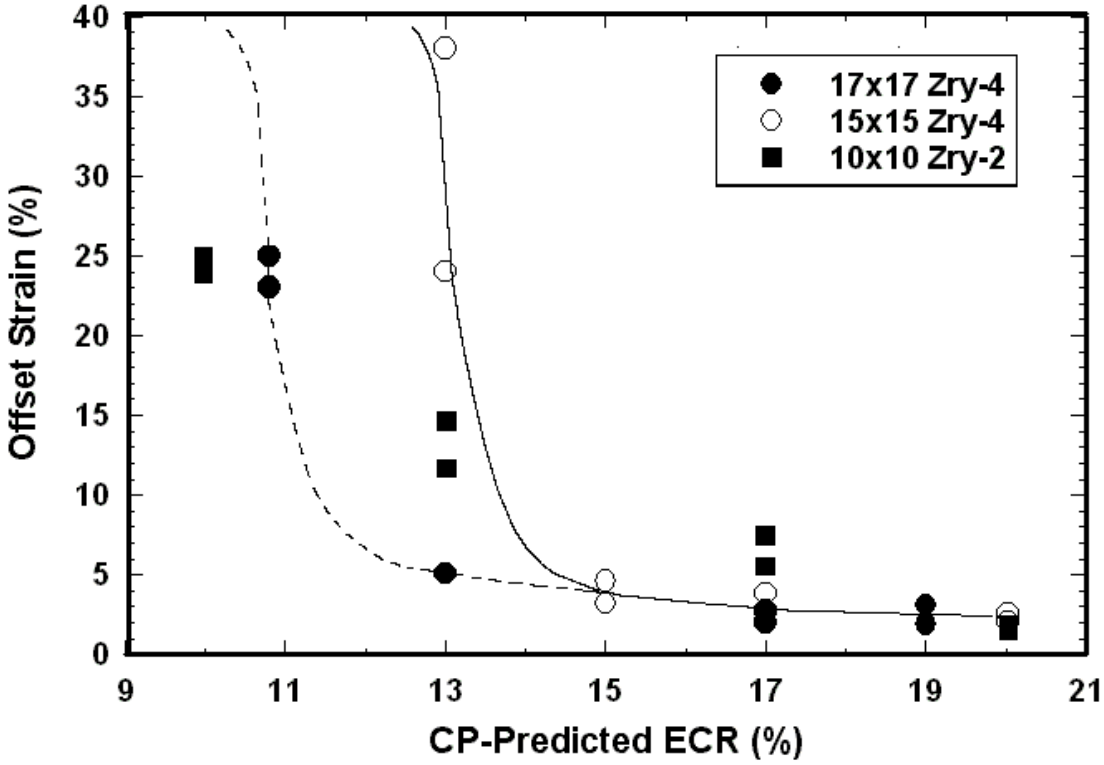

Figure 48. Post-quench ductility (offset strain) vs. CP-ECR for Westinghouse 17x17 Zry-4, AREVA 15x15 Zry-4 and 10x10 Zr-lined Zry-2, all oxidized at 1200ºC, cooled at ≈13ºC/s to 800ºC, and quenched at 800ºC. Ring-compression test temperature was 135ºC.

3.2.2 Breakaway oxidation time for 10×10 Zry-2 samples oxidized at 800-1000ºC

The breakaway oxidation time for 10×10 Zry-2 is expected to be about the same as the breakaway time for 9×9 Zry-2. One-sided oxidation tests using as-fabricated and high-burnup 9×9 Zry-2 were conducted at 1000°C for hold-times of 1200 s, 3600 s and 6000 s. Although metallographic analysis of these samples was not conducted, sample weight gains were measured for the high-burnup samples. The results from Yan et al. [22] are presented in Figure 49. Even with the artifact of some inner-surface oxidation contributing to measured weight gain, the 3600-s sample showed no evidence of breakaway oxidation. The 6000-s sample had a weight gain 25% higher than the CP-predicted weight gain. At least 10% of this can be attributed to inner-surface oxidation near the ends of the sample. The remaining 15% may be a combination of breakaway oxidation and/or additional inner-surface oxidation for such a long test time. Based on the belt-polished 15×15 Zry-4 results, the breakaway-oxidation time is expected to be ≈5000 s for belt-polished 10×10 and 9×9 Zry-2.

Two-sided breakaway oxidation tests were conducted with 10×10 Zry-2 cladding samples. Tests were run for 5000 s at 1000º±8ºC long-time hold temperature (see Figure 41). Samples were cooled to RT without quench. The tests were repeated by lowering the control temperature by 15ºC, 30ºC and 200ºC to give target temperatures of 985ºC, 970ºC and 800ºC. The test matrix is given in Table 23, along with the results for weight gain, hydrogen content and calculated hydrogen pickup. Within the temperature range of ≈960-1010ºC, the breakaway oxidation time for Zry-2 cladding is >5000 s.

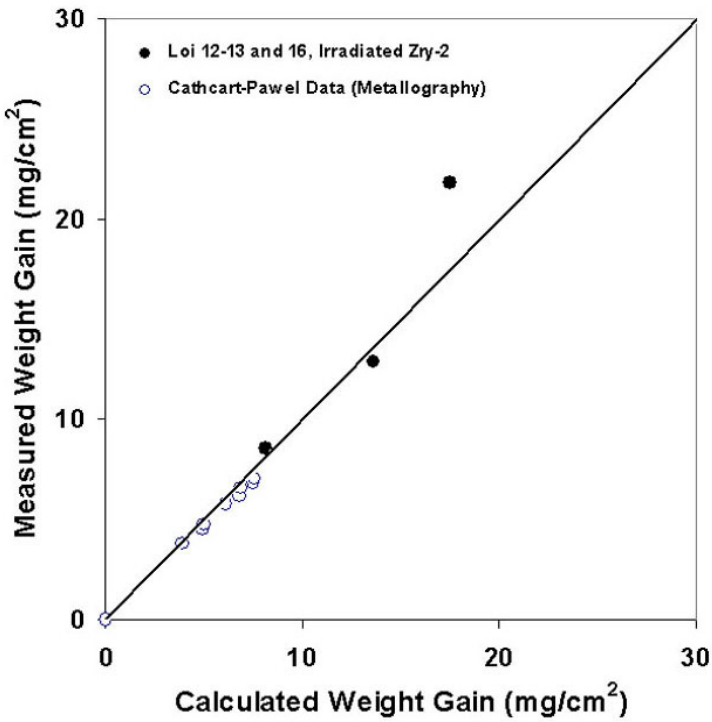

Figure 49. Comparison of Cathcart-Pawel model predictions to ANL sample weight gain data for irradiated (Limerick) Zry-2 after steam oxidation at ≈1000˚C for test times of 1200 s, 3600 s and 6000 s.

Table 23 Test Matrix and Results for Breakaway Oxidation Studies of 10x10 Zry-2 Cladding; test times are given from the beginning of the ramp from 300ºC to the end of the hold time at temperature

Oxidation T ºC	Test Time, s	Weight Gain, mg/cm^2		H-Content wppm	H-pickup[a] wppm	Outer-Surface
		CP	Measured			
1000±8	5000	15.6	12.1	16	4	Lustrous Black
1000±8[b]	**5000**	**15.6**	**11.5**	**32**	**21**	**Lustrous Black**
985±8	5000	14.4	9.8	27	15	Lustrous Black
970±8	5000	13.1	8.7	15	3	Lustrous Black
800	5000	{TBD}	{TBD}	{TBD}	{TBD}	{TBD}

[a]Hydrogen pickup (ΔC_H) is referenced to the as-fabricated weight of the sample and is calculated from $\Delta C_H = (1 + 4.7\times10^{-3}\ Wg)\ L_H - C_{Hi}$, where Wg is the measured weight gain in mg/cm^2. C_{Hi}, is 13 wppm.
[b]20-µm-deep scratch was fabricated along the length of the sample prior to testing.